NASA/TM—1998-207920

AIAA–98–0000

Thermal State-of-Charge in Solar Heat Receivers

Carsie A. Hall, III, Emmanuel K. Glakpe, and Joseph N. Cannon
Howard University, Washington DC

Thomas W. Kerslake
Lewis Research Center, Cleveland, Ohio

Prepared for the
36th Aerospace Sciences Meeting & Exhibit
sponsored by the American Institute of Aeronautics and Astronautics
Reno, Nevada, January 12–15, 1998

National Aeronautics and
Space Administration

Lewis Research Center

June 1998

Acknowledgments

The financial support of the NASA Lewis Research Center to Howard University under grant number NAG3–1907 is gratefully acknowledged.

Available from

NASA Center for Aerospace Information
800 Elkridge Landing Road
Linthicum Heights, MD 21090-2934
Price Code: A03

National Technical Information Service
5287 Port Royal Road
Springfield, VA 22100
Price Code: A03

THERMAL STATE-OF-CHARGE IN SOLAR HEAT RECEIVERS

Carsie A. Hall, III*, Emmanuel K. Glakpe†, and Joseph N. Cannon‡
College of Engineering, Architecture and Computer Sciences
Howard University, Washington, D.C. 20059
and
Thomas W. Kerslake§
NASA Lewis Research Center, Cleveland, Ohio 44135

A theoretical framework is developed to determine the so-called *thermal state-of-charge (SOC)* in solar heat receivers employing encapsulated phase change materials (PCMs) that undergo cyclic melting and freezing. The present problem is relevant to space solar dynamic power systems that would typically operate in low-Earth-orbit (LEO). The solar heat receiver is integrated into a closed-cycle Brayton engine that produces electric power during sunlight and eclipse periods of the orbit cycle. The concepts of available power and virtual source temperature, both on a finite-time basis, are used as the basis for determining the *SOC*. Analytic expressions for the available power crossing the aperture plane of the receiver, available power stored in the receiver, and available power delivered to the working fluid are derived, all of which are related to the *SOC* through *measurable parameters*. Lower and upper bounds on the *SOC* are proposed in order to delineate absolute limiting cases for a range of input parameters (orbital, geometric, etc.). *SOC* characterization is also performed in the subcooled, two-phase, and superheat regimes. Finally, a previously-developed physical and numerical model of the solar heat receiver component of NASA Lewis Research Center's Ground Test Demonstration (GTD) system is used in order to predict the *SOC* as a function of *measurable parameters*.

Nomenclature

A	= area or growth constant
c	= specific heat of solid or liquid PCM
c_p	= specific heat of working fluid
D_{cav}	= active cavity diameter
D_{ap}	= aperture diameter
F	= geometric view factor
h	= enthalpy per unit mass
h_{sf}	= PCM latent heat of fusion
H	= Heaviside function
$\dot{m}$	= working fluid mass flow rate
M	= total number of axial nodes along tube or total PCM mass
N	= total number of tubes in receiver
p	= working fluid pressure
$\dot{Q}$	= heat transfer rate
R	= gas constant
s,S	= specific, total entropy
$\dot{S}_{gen}$	= entropy generation rate
Ste	= Stefan number
t	= time
T	= temperature
T_m	= PCM melting temperature
T_o	= environmental dead state temperature
T_p,T_l	= sunset, sunrise temperature
T*	= virtual source temperature
u,U	= specific, total internal energy
V	= total volume
$\dot{W}$	= rate of work transfer
z	= axial location
β_1	= first conjugate *SOC* function
β_2	= second conjugate *SOC* function
χ_j	= jth tube mass fraction
ε	= thermal capacitance ratio
Φ	= primary *SOC* function
γ	= ratio of specific heats
ρ	= density
σ	= Stefan-Boltzmann constant
τ_{on},τ_{off}	= sun period, eclipse period
τ_{cyc}	= total orbit period

Subscripts

avg	= average
in, out	= tube inlet, tube outlet
losses	= losses through shell and aperture
min,max	= minimum, maximum
rcvr	= receiver

*Doctoral Candidate, Department of Mechanical Engineering. Student Member AIAA.

† Professor, Department of Mechanical Engineering. Member AIAA.

‡ Professor, Department of Chemical Engineering.

§Power Systems Engineer.

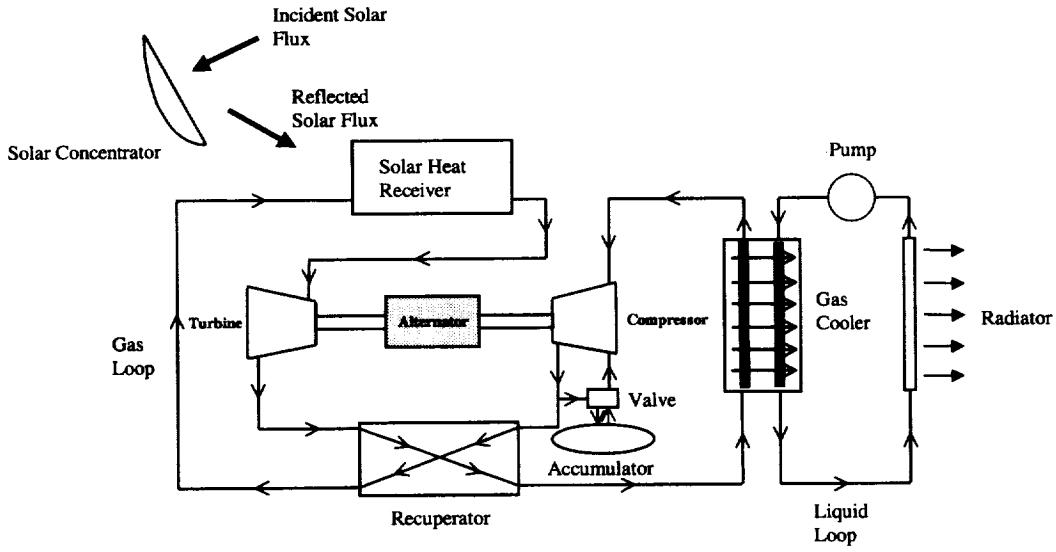

Fig. 1 Thermodynamic cycle for closed Brayton engine integrated with solar heat receiver.

Introduction

SOLAR heat receivers are very critical components in the production of electric power via solar dynamic power systems (SDPSs). During operation, the SDPS uses: 1) a concentrator to collect and focus the incident energy onto the aperture plane of a central receiver, 2) a central receiver to collect and distribute, with minimal losses, the reflected energy from the concentrator, 3) working fluid tubes aligned along the periphery of the receiver to absorb the distributed energy as heat, thus, raising the temperature of the working fluid (typically a low-Prandtl-number fluid) flowing through the tubes, 4) a turbine to expand the high temperature working fluid to produce mechanical work via a rotating shaft, 5) a compressor to circulate the working fluid through the working fluid tubes, and 6) an alternator to convert mechanical shaft motion into electric power. A recuperator is often added to increase the thermal efficiency of the thermodynamic cycle (typically a closed Brayton cycle as depicted in Fig. 1).

Solar heat receivers employing encapsulated phase change materials (PCMs) have the advantage over sensible heat receivers of requiring less mass while producing higher energy storage densities. This, in turn, makes them ideal candidates for energy storage in the space environment where temperatures are sufficiently high and PCMs with high latent heats of fusion become indispensable.

In this paper, a theoretical framework on the so-called *thermal state-of-charge (SOC)* of solar heat receivers employing latent heat thermal energy storage (LHTES) is developed. The instantaneous amount of phase change material (PCM) in the liquid phase was identified by Strumpf et al.[1] as an indicator of the *SOC*. This definition, however, is a better indicator of PCM effectiveness or some performance measure (e.g. efficiency) of the receiver as it relates to incorporating phase change storage. It may also be tempting to define the *SOC* as the instantaneous amount of energy stored in the receiver. According to NASA[2], "*Techniques are needed to determine the so-called receiver state of charge, or the quantity of stored thermal energy within the receiver.*" However, this idea can be quickly dismissed on second law grounds since energy quality can be considered a factor in determining the true *SOC*. It should be pointed out that the issue of energy quality does not adhere to conservation principles. In other words, the statement *conservation of entropy* has no meaning since all real devices that undergo energy exchange processes are involved in the one-way production of entropy. In what follows, it will be shown that the available power stored in the receiver is related to a newly-defined, time-dependent *SOC* function, which may be completely characterized by *measurable parameters*. Knowledge of the *SOC* allows for better control strategies relating to power management schemes during such operations as peak power demand and emergency shutdowns with subsequent restarts. It also helps to better identify the energy startup characteristics of the solar heat receiver in relation to the entire solar dynamic (SD) system, which ensures safe operation of the SD system through all modes and regimes of operation.

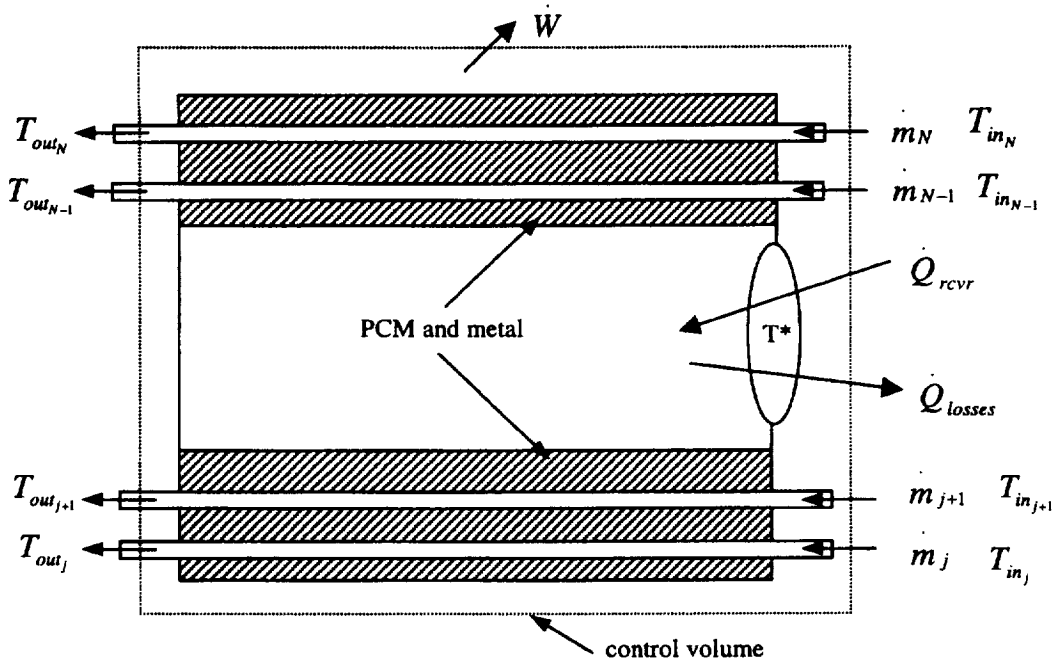

Fig. 2 Solar heat receiver available power and *SOC* model indicating control volume.

Theoretical Framework

Solar Heat Receiver Available Power

By definition, the available power of any device is the maximum rate at which energy may be extracted by a work transfer interaction if the device is allowed to come into total (thermal, mechanical, chemical) equilibrium with its surroundings at some dead state.[3] Shown in Fig. 2 is the model (including control volume) used to derive an expression for the available power stored in the receiver. A 1st law energy balance on the entire receiver with a single fluid stream results in the following:

$$\dot{W} = \left(\dot{m}h\right)_{in} - \left(\dot{m}h\right)_{out} + \dot{Q}_{rcvr} - \dot{Q}_{losses} - \frac{\partial U}{\partial t} \quad (1)$$

where $\dot{W}$ is the rate of work transfer across the boundary of the control volume (this is what could be theoretically extracted if the receiver was connected to a work-extracting mechanism), $\dot{m}$ is the working fluid mass flow rate, h is the enthalpy per unit mass of the working fluid, $\dot{Q}_{rcvr}$ is the rate at which energy crosses the aperture plane, $\dot{Q}_{losses}$ is the rate at which energy leaves the receiver due to reradiation from the canister surfaces back out through the aperture and conduction losses through the receiver shell, and U is the total internal energy of the receiver. An associated entropy balance results in

$$\frac{\partial S}{\partial t} = \left(\dot{m}s\right)_{in} - \left(\dot{m}s\right)_{out} + \frac{\dot{Q}_{rcvr}}{T^*} - \frac{\dot{Q}_{losses}}{T_o} + \dot{S}_{gen} \quad (2)$$

where S is the total entropy of the receiver, s is the entropy per unit mass of the working fluid, T* is a virtual source or effective aperture temperature (defined in the next section), T_o is the environmental dead state temperature, and $\dot{S}_{gen}$ is the rate of entropy generation inside the receiver. Subsequently eliminating the power loss term between Eqs. 1 and 2 gives

$$\dot{W} = \left[\dot{m}(h - T_o s)\right]_{in} - \left[\dot{m}(h - T_o s)\right]_{out} + \dot{Q}_{rcvr}\left(1 - \frac{T_o}{T^*}\right) - T_o \dot{S}_{gen} - \frac{\partial}{\partial t}(U - T_o S) \quad (3)$$

in which the maximum is

$$W_{max} = \left[\dot{m}(h - T_o s)\right]_{in} - \left[\dot{m}(h - T_o s)\right]_{out} + \dot{Q}_{rcvr}\left(1 - \frac{T_o}{T^*}\right) - \frac{\partial}{\partial t}(U - T_o S) \quad (4)$$

since $\dot{S}_{gen} = 0$ for a receiver operating reversibly. Now, it is assumed that the specific enthalpy in Eq. 4 is a function of temperature and pressure, i.e.

$$h = h(T,p) \quad (5)$$

and the specific entropy is a function of specific enthalpy and pressure, i.e.

$$s = s(h,p) \quad (6)$$

which for changes in specific enthalpy and specific entropy results in

$$dh = \left.\frac{\partial h}{\partial T}\right|_p dT + \left.\frac{\partial h}{\partial p}\right|_T dp \quad (7)$$

$$ds = \left.\frac{\partial s}{\partial h}\right|_p dh + \left.\frac{\partial s}{\partial p}\right|_h dp \quad (8)$$

Through the use of Maxwell's relations, ideal gas assumptions for the working fluid, and the definition of specific heat at constant pressure, it can be shown that Eqs. 7 and 8 when integrated from inlet conditions to outlet conditions yield

$$h_{out} - h_{in} = c_p\left(T_{out} - T_{in}\right) \quad (9)$$

$$s_{out} - s_{in} = c_p \ln\left(\frac{T_{out}}{T_{in}}\right) - R\ln\left(\frac{p_{out}}{p_{in}}\right) \quad (10)$$

For a solar heat receiver with N tubes (see Fig. 2), the available power is written as

$$W_{max} = -\left\{\sum_{j=1}^{N} \dot{m}_j c_p\left[\left(T_{out} - T_{in}\right)_j - T_o \ln\left(\frac{T_{out}}{T_{in}}\right)_j + T_o\left(\frac{\gamma-1}{\gamma}\right)\ln\left(\frac{P_{out}}{P_{in}}\right)_j\right]\right\} + \dot{Q}_{rcvr}\left(1 - \frac{T_o}{T^*}\right) - \frac{\partial}{\partial t}(U - T_o S) \quad (11)$$

where upon defining the jth tube mass fraction as

$$\chi_j = \frac{\dot{m}_j}{\sum_{i=1}^{N}\dot{m}_i} \text{ such that } \dot{m} = \sum_{i=1}^{N}\dot{m}_i \text{ and } \sum_{j=1}^{N}\chi_j = 1 \quad (12)$$

Eq. 11 can be expressed in non-dimensional form as

$$\frac{W_{max}}{\dot{m}c_p T_o} = -\left\{\sum_{j=1}^{N}\chi_j\left[\left(\frac{T_{out}}{T_o} - \frac{T_{in}}{T_o}\right)_j - \ln\left(\frac{T_{out}}{T_{in}}\right)_j + \left(\frac{\gamma-1}{\gamma}\right)\ln\left(\frac{P_{out}}{P_{in}}\right)_j\right]\right\} + \frac{\dot{Q}_{rcvr}}{\dot{m}c_p T_o}\left(1 - \frac{T_o}{T^*}\right) - \frac{1}{\dot{m}c_p T_o}\frac{\partial}{\partial t}(U - T_o S) \quad (13)$$

in which c_p is the working fluid specific heat at constant pressure, γ is the ratio of specific heats (c_p/c_v), P_{out} is outlet pressure, and P_{in} is inlet pressure. Furthermore, the internal energy U and entropy S are given, respectively, by

$$U = \sum_{j=1}^{N}\sum_{i=1}^{4}\iiint_{V_{ij}}(\rho u)_{ij}\, dV_{ij} \quad (14)$$

and

$$S = \sum_{j=1}^{N}\sum_{i=1}^{4}\iiint_{V_{ij}}(\rho s)_{ij}\, dV_{ij} \quad (15)$$

in which the integration takes place over the ith region and jth tube. Upon further defining the dimensionless parameters

$$\dot{Q}^*_{rcvr} = \frac{\dot{Q}_{rcvr}}{\frac{T_o}{T_m}\frac{h_{sf}M}{\tau_{cyc}}},\ U^* = \frac{U}{\frac{T_o}{T_m}h_{sf}M},\ S^* = \frac{S}{\frac{h_{sf}}{T_m}M},$$
$$t^* = \frac{t}{\tau_{cyc}},\ T^*_{out} = \frac{T_{out}}{T_o},\ T^*_{in} = \frac{T_{in}}{T_o}, \text{ and } T^{**} = \frac{T^*}{T_o} \quad (16)$$

where $\tau_{cyc} = \tau_{on} + \tau_{off}$, the following dimensionless receiver available power results:

$$\frac{W_{max}}{\dot{m}c_p T_o} = -\left\{\sum_{j=1}^{N}\chi_j\left[\left(T^*_{out} - T^*_{in}\right)_j - \ln\left(\frac{T^*_{out}}{T^*_{in}}\right)_j + \left(\frac{\gamma-1}{\gamma}\right)\ln\left(\frac{P_{out}}{P_{in}}\right)_j\right]\right\} + \left(\frac{Mc}{\dot{m}c_p\tau_{cyc}}\right)\left(\frac{1}{Ste}\right)\dot{Q}^*_{rcvr}\left(1 - \frac{1}{T^{**}}\right) - \frac{\partial}{\partial t^*}\left(U^* - S^*\right) \quad (17)$$

where $Ste = cT_m / h_{sf}$ is the Stefan number, which is the ratio of PCM sensible heat to latent heat, and the ratio

$Mc/\left(\dot{m}\tau_{cyc}c_p\right)$ is the thermal capacitance ratio expressing the relative amounts of sensible heat capacity of the PCM to sensible heat capacity of the working fluid. In addition, the dimensionless available power equation can be interpreted physically as follows: the first bracketed term is the available power loss from the receiver to the gas; the second term is the available power gain by the receiver due to the net heat interaction across the aperture plane; the last term is the available power loss or gain due to unsteady charging and discharging. Furthermore, an interesting comparison can be made between the fraction of incident power available at the aperture plane, expressed in Eq. 17 as

$$\psi = 1 - \frac{T_o}{T^*} = 1 - \frac{1}{T^{**}} \tag{18}$$

and that which is reported in Moynihan[4], i.e.

$$\psi' = 1 - \frac{4}{3}\frac{T_o}{T^*} + \frac{1}{3}\left(\frac{T_o}{T^*}\right)^4 = 1 - \frac{4}{3}\frac{1}{T^{**}} + \frac{1}{3}\left(\frac{1}{T^{**}}\right)^4 \tag{19}$$

A more detailed graphic comparison is shown in Fig. 3. It should be pointed out that over the anticipated region of operation ($0.1 \le T_o/T^* \le 0.3$) the agreement is good.

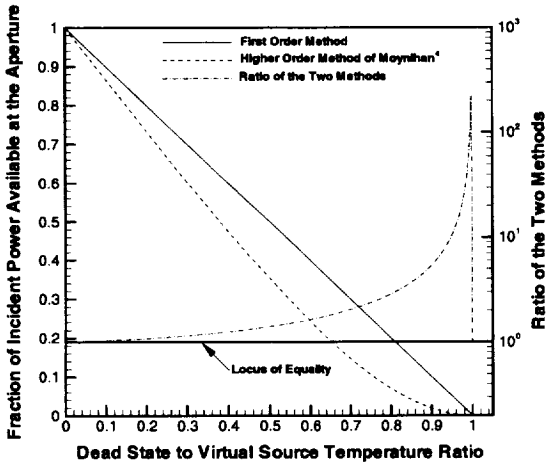

Fig. 3 Comparison of the fraction of incident power available at the aperture as a function of the ratio of dead state temperature and virtual source temperature.

Virtual Source Temperature

The effective temperature of the aperture due to the net heat interaction across the aperture plane is defined as the virtual source temperature. It expresses continuity of energy reradiated from the outer surfaces of the canisters to the aperture. Therefore, an energy balance on the aperture plane of the receiver shown in Fig. 2 results in

$$\sum_{j=1}^{M+1} A_j F_{j-ap}\sigma\left[T_j^4(t) - T^{*4}(t)\right] = A_{ap}F_{ap-o}\sigma\left[T^{*4}(t) - T_o^4\right] \tag{20}$$

where upon solving for the virtual source temperature T* gives

$$T^*(t) = \left\{\frac{A_{ap}F_{ap-o}\sigma T_o^4 + \sum_{j=1}^{M+1} A_j F_{j-ap}\sigma T_j^4(t)}{A_{ap}F_{ap-o}\sigma + \sum_{j=1}^{M+1} A_j F_{j-ap}\sigma}\right\}^{\frac{1}{4}} \tag{21}$$

which in dimensionless form is written as

$$T^{**}(t^*) = \frac{T^*(t^*)}{T_o} = \left\{\frac{1 + \sum_{j=1}^{M+1}\frac{A_j}{A_{ap}}\frac{F_{j-ap}}{F_{ap-o}}T_j^{*4}(t^*)}{1 + \sum_{j=1}^{M+1}\frac{A_j}{A_{ap}}\frac{F_{j-ap}}{F_{ap-o}}}\right\}^{\frac{1}{4}} \tag{22}$$

In Eq. 22, the jth area ratio (A_j/A_{ap}) can be written as

$$\frac{A_j}{A_{ap}} = \frac{\pi D_{cav}\Delta z}{\frac{\pi}{4}D_{ap}^2} = 4\left(\frac{D_{cav}}{D_{ap}}\right)\left(\frac{\Delta z}{D_{ap}}\right) \tag{23}$$

Notice that Eq. 23 contains one of the cavity aspect ratios (D_{cav}/D_{ap}), which is a key parameter that affects the thermal performance of the solar heat receiver. Also, the geometric view factors in Eqs. 20-22 are given by analytic expressions found in Howell.[7]

Gas Available Power

Recall the expression given by Eq. 11, which is the instantaneous available power stored in the receiver. It should be pointed out here that the first term in brackets in Eq. 11 represents the instantaneous available power of the gas before mixing in the outlet manifold. This power, which is the difference between the enthalpy transferred to gas and a term proportional to the entropy transferred to the gas, is rewritten here as

$$W_{gas} = \sum_{j=1}^{N} m_j c_p\left[\left(T_{out} - T_{in}\right)_j - T_o\ln\left(\frac{T_{out}}{T_{in}}\right)_j + T_o\left(\frac{\gamma-1}{\gamma}\right)\ln\left(\frac{P_{out}}{P_{in}}\right)_j\right] \tag{24}$$

which is expressed in dimensionless form as

$$\frac{\dot{W}_{gas}}{\dot{m}c_pT_o} = \sum_{j=1}^{N}\chi_j\left\{\left(\frac{T_{out}}{T_o}-\frac{T_{in}}{T_o}\right)_j - \ln\left(\frac{T_{out}}{T_{in}}\right)_j + \left(\frac{\gamma-1}{\gamma}\right)\ln\left(\frac{P_{out}}{P_{in}}\right)_j\right\}$$

$$= \sum_{j=1}^{N}\chi_j\left\{\left(T^*_{out}-T^*_{in}\right)_j - \ln\left(\frac{T^*_{out}}{T^*_{in}}\right)_j + \left(\frac{\gamma-1}{\gamma}\right)\ln\left(\frac{P_{out}}{P_{in}}\right)_j\right\} \quad (25)$$

Physically, the reduction in available power associated with the transport of entropy to the gas can be attributed to two sources: 1) heat transfer to the gas across finite temperature differences and 2) frictional effects leading to reductions in pressure along the lengths of each of the tubes in the receiver. The concept of entropy is associated with the amount of unavailable energy within a system. Therefore, the available power of the gas, expressed by Eq. 25, is that which is delivered to the outlet manifold before any mixing takes place. Any further reduction in available power takes place in the outlet manifold due to irreversible mixing of each of the individual fluid streams. Finally, it is observed that all of the parameters in Eq. 25 can either be readily calculated or directly measured.

Mixing-Based Lost Available Power

It is known that the lost available power associated with the gas is proportional to the entropy generation rate, where the proportionality constant is the dead state temperature.[3,6] Expressed mathematically,

$$\dot{W}_{lost} = T_o\,\dot{S}_{gen} \quad (26)$$

For a solar heat receiver with N tubes and N associated fluid streams, the entropy generation rate due to irreversible fluid stream mixing in the outlet manifold is given by

$$\dot{S}_{gen} = \dot{m}s_{N+1} - \sum_{j=1}^{N}\dot{m}\chi_j s_j \quad (27)$$

which, due partly to Eq. 10, can be subsequently written in terms of temperatures as

$$\dot{S}_{gen} = \dot{m}c_p\sum_{j=1}^{N}\chi_j\ln\left(\frac{T_{N+1}}{T_j}\right) \quad (28)$$

where T_j is the fluid outlet temperature of the jth tube just before entering the outlet manifold and N+1 corresponds to mixed mean properties in the outlet manifold just before entering the turbine. The corresponding loss in available power of the gas is expressed as

$$\dot{W}_{lost} = T_o\,\dot{S}_{gen} = \dot{m}c_pT_o\sum_{j=1}^{N}\chi_j\ln\left(\frac{T_{N+1}}{T_j}\right) \quad (29)$$

which can be further written in the following non-dimensional form:

$$\frac{\dot{W}_{lost}}{\dot{m}c_pT_o} = \sum_{j=1}^{N}\chi_j\ln\left(\frac{T_{N+1}}{T_j}\right) \quad (30)$$

As expected, when each tube in the receiver is imparted with the same incident flux, the temperature of each gas stream exiting all the tubes is the same, resulting in no loss in available power. This is revealed in Eq. 30.

Relation Between *SOC* and Available Power

A dimensionless conjugate *SOC* function β_1 is defined here as the ratio of instantaneous available power stored in the receiver with no available power lost to the working fluid to minimum gas available power required to operate the turbine, or

$$\beta_1 = \frac{\dot{W}_{max}}{\dot{W}_{min}} = \frac{\left(\frac{M}{\dot{m}\tau_{cyc}}\right)\left(\frac{c}{c_p}\right)\left(\frac{1}{Ste}\right)\left\{\dot{Q}^*_{rcvr}\left(1-\frac{1}{T^{**}}\right)-\frac{\partial}{\partial t^*}\left(U^*-S^*\right)\right\}}{\sum_{j=1}^{N}\chi_j\left\{\left(T^*_{min}-T^*_{in}\right)_j - \ln\left(\frac{T^*_{min}}{T^*_{in}}\right)_j + \left(\frac{\gamma-1}{\gamma}\right)\ln\left(\frac{P_{min}}{P_{in}}\right)_j\right\}} \quad (31)$$

A second dimensionless conjugate *SOC* function β_2 is defined as the ratio of instantaneous gas available power to minimum gas available power required to operate the turbine, i.e.

$$\beta_2 = \frac{\dot{W}_{gas}}{\dot{W}_{min}} = \frac{\sum_{j=1}^{N}\chi_j\left\{\left(T^*_{out}-T^*_{in}\right)_j - \ln\left(\frac{T^*_{out}}{T^*_{in}}\right)_j + \left(\frac{\gamma-1}{\gamma}\right)\ln\left(\frac{P_{out}}{P_{in}}\right)_j\right\}}{\sum_{j=1}^{N}\chi_j\left\{\left(T^*_{min}-T^*_{in}\right)_j - \ln\left(\frac{T^*_{min}}{T^*_{in}}\right)_j + \left(\frac{\gamma-1}{\gamma}\right)\ln\left(\frac{P_{min}}{p_{in}}\right)_j\right\}} \quad (32)$$

where the outlet manifold mixing losses have been neglected in both conjugate functions for convenience. Upon further defining the denominator of Eqs. 31 and 32 as

$$\beta_{min} = \sum_{j=1}^{N}\chi_j\left\{\left(T^*_{min}-T^*_{in}\right)_j - \ln\left(\frac{T^*_{min}}{T^*_{in}}\right)_j + \left(\frac{\gamma-1}{\gamma}\right)\ln\left(\frac{P_{min}}{p_{in}}\right)_j\right\} \quad (33)$$

the conjugate *SOC* functions and β_{min} can be related to the dimensionless receiver available power (Eq. 17) as

$$\beta_{\min}(\beta_1 - \beta_2) = \frac{\dot{W}_{\max}}{\dot{m} c_p T_o} \tag{34}$$

Now, define the primary *SOC* function as the dimensionless combination

$$\Phi \equiv \frac{\beta_1 - 1}{\beta_{\max} - 1} \tag{35}$$

such that Φ is always in the range $0 \le \Phi \le 1$. Notice that β_{min} is β_2 evaluated at $T_{out} = T_{min}$ and $P_{out} = P_{min}$ and β_{max} is the maximum value that the first conjugate *SOC* function β_1 can take on, which can be shown to be

$$\beta_{\max} = \frac{\dot{W}_{\max}}{\dot{W}_{\min}} = \frac{\left(\frac{M}{\dot{m}\tau_{cyc}}\right)\left(\frac{c}{c_p}\right)\left(\frac{1}{Ste}\right)\left\{\dot{Q}^*_{rcvr}\left(1 - \frac{1}{T^{**}}\right)\right\}}{\sum_{j=1}^{N} \chi_j \left\{\left(T^*_{\min} - T^*_{in}\right)_j - \ln\left(\frac{T^*_{\min}}{T^*_{in}}\right)_j + \left(\frac{\gamma - 1}{\gamma}\right)\ln\left(\frac{P_{\min}}{P_{in}}\right)_j\right\}} \tag{36}$$

which is just the steady-state equivalent of Eq. 31. Therefore, the maximum *SOC* is achieved when the thermodynamic state of the receiver is driven to steady-state conditions even though the system is designed to operate under cyclic conditions.

Results and Discussion

The intrinsic coupling between the size (and design) of the solar heat receiver and the turbine for which it is intended to supply high temperature, high pressure gas makes it prudent to understand the minimum necessary thermodynamic requirements for operating the turbine. Mason[8] describes a process called *motoring* in which a DC electric power source is initially used to drive the turbo-alternator compressor (TAC) while the turbine is pre-heated and, ultimately, becomes self-sustaining. Mason[8] identified the cycle temperature ratio (turbine inlet/compressor inlet temperature) as the leading indicator for the time when the TAC becomes self-sustaining. It was determined that minimum motoring time is achieved as the cycle temperature ratio approaches a value of three (3) asymptotically. This information can subsequently be used to determine the minimum thermodynamic state-point (temperature and pressure) and associated minimum gas available power needed to operate the turbine. Of course, this minimum gas available power is that which is delivered from the receiver to the gas.

One important mode of operation of the solar dynamic (SD) system is the so-called balanced orbit mode (BOM) wherein measured quantities are repeatable (within allowable limits) from one sunrise to the next and from one sunset to the next. In order to describe the aforementioned minima in BOM, the gas inlet temperature profile must be specified. Owing to the cyclic nature of the solar source, thermodynamic parameters in the system responding to the cyclic solar source will also experience cyclic changes throughout the orbit cycles. It is interesting to note that the only coupling that the receiver has with the rest of the thermodynamic cycle is through the gas mass flow rate and gas inlet temperature, which is intricately coupled to the gas mass flow rate and components of the heat rejection loop (recuperator, gas coolers, radiators, heat-rejection coolant, etc.). Knowledge of these two *measurable parameters* along with the pressure drop through the tubes are all that is required to calculate the gas available power (Eq. 24). In order to model cyclic changes that occur inside the receiver in BOM, several inlet temperature test profiles are proposed:

Sawtooth:

$$T_{in}(t) = \left(T_p - T_l\right)\frac{t}{\tau_{on}} + T_l, \quad 0 \le t \le \tau_{on}$$

$$= -\left(T_p - T_l\right)\frac{t}{\tau_{off}} + \left(T_p - T_l\right)\frac{\tau_{on}}{\tau_{off}} + T_p,$$

$$\tau_{on} \le t \le \tau_{on} + \tau_{off}$$

which can be written in dimensionless form as

$$T_{in}^*(t^*) = \left(T_p^* - T_l^*\right)\left(1 + \frac{\tau_{off}}{\tau_{on}}\right)t^* + T_l^*,$$

$$0 \le t^* \le \frac{1}{1 + \frac{\tau_{off}}{\tau_{on}}}$$

$$= -\left(T_p^* - T_l^*\right)\left(1 + \frac{\tau_{on}}{\tau_{off}}\right)t^* + \left(T_p^* - T_l^*\right)\frac{\tau_{on}}{\tau_{off}} + T_p^*,$$

$$\frac{1}{1 + \frac{\tau_{off}}{\tau_{on}}} \le t^* \le 1$$

where $T^* = \frac{T}{T_o}$, $t^* = \frac{t}{\tau_{on} + \tau_{off}}$, T_p is the sunset temperature, and T_l is the sunrise temperature; T_p and T_l are repeatable from one cycle to the next in BOM.

Positive-Sine:

$$T_{in}(t) = \left(T_p - T_l\right)\left|\sin\left(\frac{\pi}{2}\frac{t}{\tau}\right)\right| + T_l, \quad 0 \le t \le 2\tau$$

which, in non-dimensional form, is expressed as

$$T_{in}^{*}(t^{*}) = \left(T_p^{*} - T_l^{*}\right)\left|\sin\left(\pi t^{*}\right)\right| + T_l^{*}, \quad 0 \le t^{*} \le 1$$

Exponential Growth / Power Law Decay (m < 0):

$$T_{in}(t) = \left(T_l - T_p\right)e^{A\left[1-\frac{\tau_{on}}{\tau_{on}-t}\right]} + T_p, \quad 0 \le t \le \tau_{on}$$

$$= \frac{\left(T_p - T_l\right)}{\tau_{on}^{m} - \left(\tau_{on} + \tau_{off}\right)^{m}}\left[t^{m} - \tau_{on}^{m}\right] + T_p, \quad \tau_{on} \le t \le \tau_{on} + \tau_{off}$$

which is written in non-dimensional form as

$$T_{in}^{*}(t^{*}) = \left(T_l^{*} - T_p^{*}\right)e^{A\left[1-\frac{1}{1-\left(1+\frac{\tau_{off}}{\tau_{on}}\right)t^{*}}\right]} + T_p^{*}, \quad 0 \le t^{*} \le \frac{1}{1+\frac{\tau_{off}}{\tau_{on}}}$$

$$= \frac{\left(T_p^{*} - T_l^{*}\right)}{\left(\frac{1}{1+\frac{\tau_{off}}{\tau_{on}}}\right)^{m} - 1}\left[t^{*m} - \left(\frac{1}{1+\frac{\tau_{off}}{\tau_{on}}}\right)^{m}\right] + T_p^{*}, \quad \frac{1}{1+\frac{\tau_{off}}{\tau_{on}}} \le t^{*} \le 1$$

For this test case, the system is allowed to reach a steady-state mode before decaying into an eclipse. The growth constant A is found by matching the initial rate of temperature rise from a previous balanced orbit mode. For the other two test profiles above, the growth constant is calculated to be

1. Sawtooth: $A = 1$

2. Positive-Sine: $A = \frac{\pi}{2}$

Figs. 4-6 illustrate the cyclic variation of minimum gas available power in response to the cyclic inlet temperature profiles outlined above.

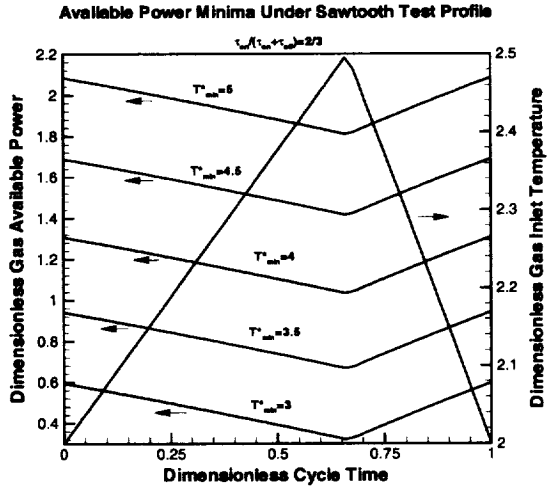

Fig. 4 Gas available power minima curves under balanced orbit conditions with a cyclic sawtooth inlet temperature profile.

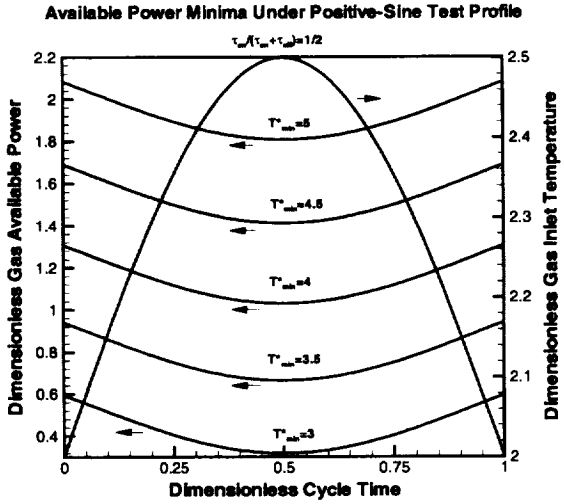

Fig. 5 Gas available power minima curves under balanced orbit conditions with a cyclic positive-sine inlet temperature profile.

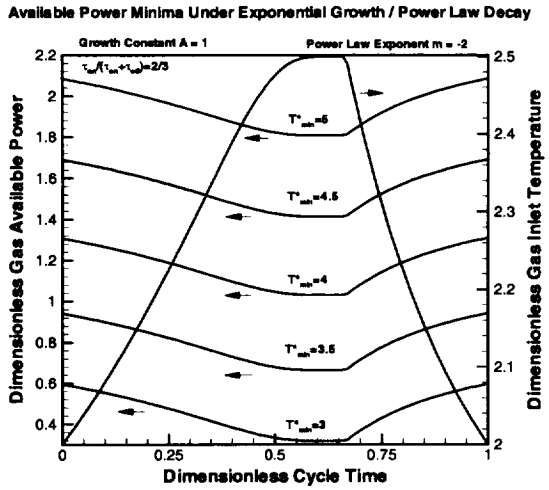

Fig. 6 Gas available power minima curves under balanced orbit conditions with a cyclic exponential growth / power law decay inlet temperature profile.

Extrema of Solar Heat Receiver *SOC*

First consider the minimum *SOC* given by

$$\Phi = 0$$

which corresponds to $\beta_1=1$. Therefore, along curves of $(\Phi,\beta_1)=(0,1)$, the following expression holds:

$$\beta_{\min}(t^*) = \frac{\varepsilon}{Ste}\dot{Q}^*_{rcvr}\left[1-\frac{T_o}{T^*(t^*)}\right] - \frac{\partial}{\partial t^*}(U^*-S^*)$$

which is integrated to

$$\left[U^*(t^*)-U^*(0)\right]-\left[S^*(t^*)-S^*(0)\right] = \int_0^{t^*}\left\{\frac{\varepsilon}{Ste}\dot{Q}^*_{rcvr}\left[1-\frac{T_o}{T^*(t^{*'})}\right]-\beta_{\min}(t^{*'})\right\}dt^{*'}$$

where ε is the thermal capacitance ratio

$$\varepsilon = \frac{Mc}{m\tau_{cyc}c_p}$$

In addition, if the system has reached a balanced orbit, then the integral of the unsteady term vanishes since U*(1) = U*(0) and S*(1) = S*(0), which results in

$$\int_0^1 \frac{\partial}{\partial t^*}(U^*-S^*)dt^* = \int_0^1\left\{\frac{\varepsilon}{Ste}\dot{Q}^*_{rcvr}\left[1-\frac{T_o}{T^*(t^*)}\right]-\beta_{\min}(t^*)\right\}dt^* = 0$$

which can be regarded as an integral constraint on the functions

$$\dot{Q}^*_{rcvr}(t^*),\ T_o/T^*(t^*),\text{ and } \beta_{\min}(t^*)$$

Now consider the maximum *SOC* given by

$$\Phi = 1$$

which corresponds to $\beta_1=\beta_{\max}$. Therefore, along curves of $(\Phi,\beta_1)=(1,\beta_{\max})$, the following expression holds:

$$\beta_{\max}\beta_{\min} = \frac{\varepsilon}{Ste}\dot{Q}^*_{rcvr}\left(1-\frac{T_o}{T^*}\right)$$

or equivalently

$$\left(\frac{\beta_{\max}}{\beta_{\min}}\right)\left(\frac{Ste}{\varepsilon}\right)\beta^2_{\min} = \dot{Q}^*_{rcvr}\left(1-\frac{T_o}{T^*}\right)$$

where physically meaningful results are obtained when

$$\frac{\beta_{\max}}{\beta_{\min}} \geq 1$$

Graphical representations of the maximum *SOC* are shown in Figs. 7-9.

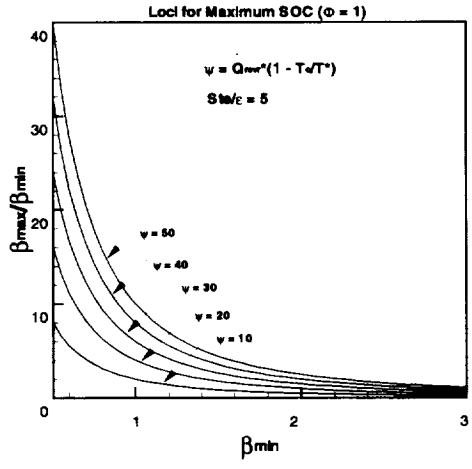

Fig. 7 Loci for maximum *SOC* as a function of minimum gas available power for selected values of receiver available power at the aperture, and a fixed combination of thermal capacity parameters.

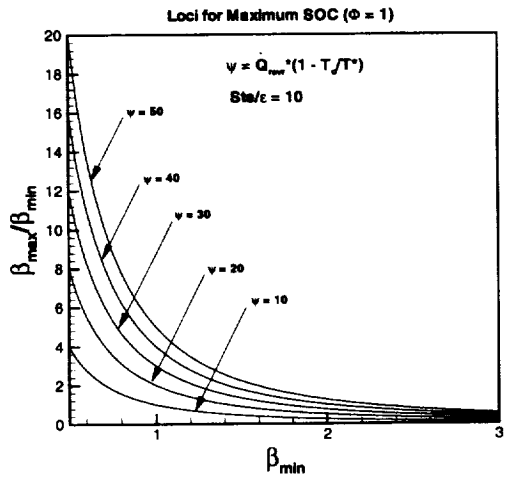

Fig. 8 Loci for maximum *SOC* as a function of minimum gas available power for selected values of receiver available power at the aperture, and a fixed but higher combination of thermal capacity parameters.

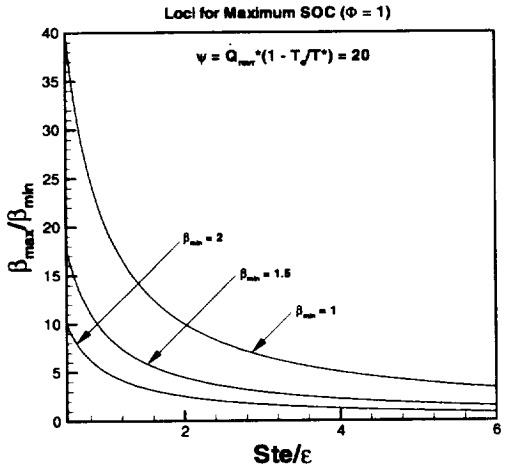

Fig. 9 Loci for maximum *SOC* as a function of a combination of thermal capacity parameters for selected values of the minimum gas available power, and a fixed value for receiver available power at the aperture.

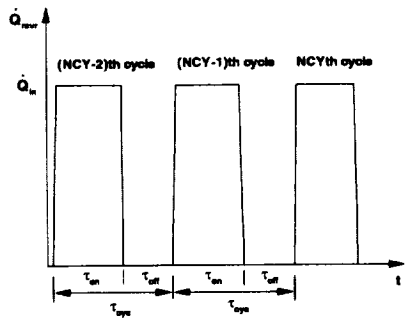

Fig. 10 Qualitative illustration of temporal variation of incident power crossing the aperture plane.

Recall that these *SOC* maxima curves correspond to an SD system operating in steady-state mode (SSM). For example, this mode can be induced by boosting the spacecraft into higher orbital altitudes, which extends the sun period and reduces the eclipse period. As might be expected, the extended sun period drives the SD system in general and the solar heat receiver in particular to a state of thermodynamic equilibrium wherin the various temperature (and other *measurable parameters*) transients are damped out. Fig. 10 shows in a qualitative sense the temporal variation of incident power entering the receiver. The discontinuity shown at the beginning of each eclipse is not a real effect since the actual transition from the sun phase into the eclipse phase is a rapid continuous decay, rather than a sharp discontinuous drop. However, it is a computationally convenient way to model the transition from sun phase to eclipse phase. Furthermore, it can be shown that the profile shown in Fig. 10 can be generated by a function given by

$$\dot{Q}_{rcvr}(t) = \sum_{j=1}^{NCY} \dot{Q}_{in_j} \left\{ H\left(t - \sum_{i=0}^{j-1} \tau_{cyc_i} \right) - H\left[t - \left(\sum_{i=0}^{j-1} \tau_{cyc_i} + \tau_{on_j} \right) \right] \right\}$$

where $\tau_0 = 0$, NCY is the total number of orbit cycles, and H is the Heaviside function. In addition, notice that the subscripted parameters allow for variations from

cycle to cycle. These variations may be due to the need for increased power level, decreased power level, increased sun period, or extended eclipse period. In addition, the incident power across the aperture may be, in general, time-dependent due to time-varying shadowing effects on the concentrator or other short transients such as concentrator mis-pointing due to plume loads from reaction control jets and/or gravity-gradient effects.[2]

As pointed out in Hall, III et al.[5] and Mason,[8] the anticipated amount of incident power crossing the aperture plane is approximately 12.5 kW, and for the orbital altitude corresponding to 250 nmi, the total orbit period is 93 minutes with about 66 minutes of sun exposure and 27 minutes of eclipse. In NASA's Ground Test Demonstration (GTD) system, the solar heat receiver uses a eutectic mixture of LiF-CaF_2 as the PCM (total mass of 53 lb_m or 24.04 kg, heat of fusion of 340 Btu/lb_m or 790 kJ/kg, and melting point of 1873 R or 1040 K) and a low-Prandlt-number (for a gas) mixture of He/Xe for the working fluid (molecular weight of 83.8, c_p = 0.059 Btu/lb_m/R), the properties of which are approximated using ideal gas assumptions. The TAC of the Brayton engine is capable of reaching speeds of up to 58,000 RPM, with a corresponding He/Xe mass flow rate of up to 0.36 lb_m/s or 163.3 g/s. These numbers correspond to a thermal capacitance ratio of $\varepsilon \cong 0.2106$, Stefan number of Ste $\cong$ 2.6, and dimensionless incident power across the aperture of approximately 13.54, assuming a dead state temperature of 360 R or 200 K. Also, note that the ratio of Stefan number to thermal capacitance ratio is Ste/$\varepsilon \cong 12.3$. The only other unknown parameter is the virtual source or effective cavity temperature, which is a nonlinear function of cavity geometric parameters and canister surface temperatures.

Ultimately, these parameters are used to determine the maximum *SOC* corresponding to β_{max} once the turbine requirements are known through the necessary minimum gas available power.

Conclusions

The theoretical framework for the determination of the *thermal state-of-charge (SOC)* in solar heat receivers employing encapsulated phase change storage has been developed. The concepts of available power, virtual source temperature, and minimum gas available power have been used in the underlying theoretical analyses. In addition, qualitative and quantitative descriptions of minimum and maximum *SOC* have been presented parametrically. Similar parametric curves can be generated for non-extremum *SOC*.

References

[1]Strumpf, H., Avanessian, V., and Ghafourian, R., "Design Analysis and Containment Canister Life Prediction for a Brayton Engine Solar Receiver for Space Station," ASME *Journal of Solar Energy Engineering*, Vol. 116, 1994, pp. 142-147.

[2]Jeffries, K.S. (ed.), "Solar Dynamic Power System Development for Space Station *Freedom*," NASA Reference Publication 1310, July 1993.

[3]Bejan, A., *Entropy Generation Through Heat and Fluid Flow*, John Wiley, New York, 1982.

[4]Moynihan, P.I., "Second-Law Efficiency of Solar-Thermal Cavity Receivers," JPL Publication 83-97, 1983.

[5]Hall, III, C.A., Glakpe, E.K., Cannon, J.N., and Kerslake, T.W., "Modeling Cyclic Phase Change and Energy Storage in Solar Heat Receivers," *Proceedings of the 32nd AIAA Thermophysics Conference*, Atlanta, Georgia, June 1997.

[6]Bellecci, C. and Conti, M., "Phase Change Energy Storage: Entropy Production, Irreversibility, and Second Law Efficiency," *Solar Energy*, Vol. 53, No. 2, 1994, pp. 163-170.

[7]Howell, J.R., *a catalog of Radiation Configuration Factors*, McGraw-Hill, New York, 1982.

[8]Mason, L.S., "Solar Dynamic Power System Test Results," M.S. Thesis, Cleveland State University, Cleveland, Ohio, 1996.

REPORT DOCUMENTATION PAGE

Form Approved
OMB No. 0704-0188

1. AGENCY USE ONLY (*Leave blank*)	2. REPORT DATE	3. REPORT TYPE AND DATES COVERED
	June 1998	Technical Memorandum

4. TITLE AND SUBTITLE

Thermal State-of-Charge in Solar Heat Receivers

5. FUNDING NUMBERS

WU-547-10-41-00

6. AUTHOR(S)

Carsie A. Hall, III, Emmanuel K. Glakpe, Joseph N. Cannon, and Thomas W. Kerslake

7. PERFORMING ORGANIZATION NAME(S) AND ADDRESS(ES)

National Aeronautics and Space Administration
Lewis Research Center
Cleveland, Ohio 44135-3191

8. PERFORMING ORGANIZATION REPORT NUMBER

E-11203

9. SPONSORING/MONITORING AGENCY NAME(S) AND ADDRESS(ES)

National Aeronautics and Space Administration
Washington, DC 20546-0001

10. SPONSORING/MONITORING AGENCY REPORT NUMBER

NASA TM—1998-207920
AIAA-98-0000

11. SUPPLEMENTARY NOTES

Prepared for the 36th Aerospace Sciences Meeting & Exhibit sponsored by the American Institute of Aeronautics and Astronautics, Reno, Nevada, January 12–15, 1998. Carsie A. Hall, III, Emmanuel K. Glakpe, and Joseph N. Cannon, College of Engineering, Architecture and Computer Sciences, Howard University, Washington, DC 20059; Thomas W. Kerslake, NASA Lewis Research Center. Responsible person, Thomas W. Kerslake, organization code 6920, (216) 433–5373.

12a. DISTRIBUTION/AVAILABILITY STATEMENT

Unclassified - Unlimited
Subject Category: 20 Distribution: Nonstandard

This publication is available from the NASA Center for AeroSpace Information, (301) 621–0390.

12b. DISTRIBUTION CODE

13. ABSTRACT (***Maximum 200 words***)

A theoretical framework is developed to determine the so-called *thermal state-of-charge* (*SOC*) in solar heat receivers employing encapsulated phase change materials (PCMs) that undergo cyclic melting and freezing. The present problem is relevant to space solar dynamic power systems that would typically operate in low-Earth-orbit (LEO). The solar heat receiver is integrated into a closed-cycle Brayton engine that produces electric power during sunlight and eclipse periods of the orbit cycle. The concepts of available power and virtual source temperature, both on a finite-time basis, are used as the basis for determining the *SOC*. Analytic expressions for the available power crossing the aperture plane of the receiver, available power stored in the receiver, and available power delivered to the working fluid are derived, all of which are related to the *SOC* through *measurable parameters*. Lower and upper bounds on the *SOC* are proposed in order to delineate absolute limiting cases for a range of input parameters (orbital, geometric, etc.). *SOC* characterization is also performed in the subcooled, two-phase, and superheat regimes. Finally, a previously-developed physical and numerical model of the solar heat receiver component of NASA Lewis Research Center's Ground Test Demonstration (GTD) system is used in order to predict the *SOC* as a function of *measurable parameters*.

14. SUBJECT TERMS

Heat storage; Phase change materials; Solar dynamic power systems; Solar energy

15. NUMBER OF PAGES

17

16. PRICE CODE

A03

17. SECURITY CLASSIFICATION OF REPORT	18. SECURITY CLASSIFICATION OF THIS PAGE	19. SECURITY CLASSIFICATION OF ABSTRACT	20. LIMITATION OF ABSTRACT
Unclassified	Unclassified	Unclassified	